NANO LETTERS

2005
Vol. 5, No. 2
339−343

Imperfect Perfect Lens

Ivan A. Larkin and Mark I. Stockman*

Department of Physics and Astronomy, Georgia State University, Atlanta, Georgia 30303

Received December 9, 2004; Revised Manuscript Received January 12, 2005

ABSTRACT

We have quantitatively established a fundamental limitation on the ultimate spatial resolution of the perfect lens (thin metal slab) in the near field. This limitation stems from the spatial dispersion of the dielectric response of the Fermi liquid of electrons with Coulomb interaction in the metal. We discuss possible applications in nanoimaging, nanophotolithography, and nanospectroscopy.

The Veselago lens,[1] that is a slab of a left-handed material with relative dielectric permittivity $\epsilon = -1$ and magnetic permeability $\mu = -1$, builds a perfect image of a three-dimensional object in the far-field zone. Such a lens was experimentally confirmed in the microwave spectral region.[2] As shown by Pendry, the same slab builds also a perfect three-dimensional image in the near field, deserving the name of perfect lens,[3] as observed later in ref 4. In the near zone, the requirement for the permeability is lifted, and only the condition of $\epsilon = -1$ is important.

Actually, such a lens is only near-perfect,[3] because its spatial resolution is limited by the losses in the lens's material; in the visible range the best material is silver, having the lowest losses. One of the points of this letter is to suggest that such losses can be minimized by using a high-index embedding dielectric that would shift the operational frequency toward the red where the quality factor of silver is much higher.[5] Light amplification can also be used to compensate these losses.[6]

In this letter, we investigate a principal limitation on the resolution of the perfect lens stemming from the spatial dispersion (nonlocality) of the dielectric response of the Fermi liquid of interacting electrons in the nanolens material. Such dispersion leads to the aberrations of this lens in the wave vector in the plane of the slab. This principally limits the resolution of this lens, making it imperfect on the scale below ~5 nanometers. This effect is independent from the known sources of the lens imperfection due to optical losses in the metal and temporal dispersion that is related to these losses by Kramers−Kronig relations. Even if the absorption is reduced or compensated by the optical gain as in ref 6, the spatial dispersion will remain and limit the resolution.

The principal role of spatial dispersion of the surface polaritons at high wavenumbers was pointed out two years ago in preprint[7] where it was considered for left-handed ($\epsilon < 0$ and $\mu < 0$) systems. Only a generic electromagnetic spectrum was considered, and no quantitative limitations on the spatial resolution were obtained, in contrast to the present letter.

We consider only near-field imaging and therefore use the quasistatic approximation, which does not include magnetic field. Therefore, the left-handedness of the material is irrelevant. Consider a metal ($\epsilon < 0$) slab of thickness b parallel to the xy plane of the coordinate system, whose boundaries are at $z = 0$ and $z = b$. Let there be a unit charge at a point $(0, 0, -a)$. Then the electric potential to the right of the slab ($z > b$) is given by[8]

$$\varphi(r, z) = 4\epsilon\int_0^\infty \frac{J_0(k_r r)e^{-k_r(z+a-2b)}}{(1+\epsilon)^2 e^{2k_r b} - (1-\epsilon)^2}\,\mathrm{d}k_r \qquad (1)$$

where ϵ is the metal permittivity relative to the host medium, J_0 is a Bessel function, $r = \sqrt{x^2+y^2}$ is the radial coordinate, and k_r is a two-dimensional (2D) wave vector in the plane of the slab. For $\epsilon = -1$ (i.e., for the frequency of the surface plasmon resonance of the metal), behind the image plane of $z \geq 2b - a$, this potential is an ideal three-dimensional (3D) image of the original single point charge

$$\varphi(r, z) = \int_0^\infty J_0(k_r r)e^{-k_r(z+a-2b)}\,\mathrm{d}k_r = \frac{1}{\sqrt{r^2 + (z-2b+a)^2}} \qquad (2)$$

If ϵ is not exactly equal to -1, e.g., due to $\mathrm{Im}\epsilon \neq 0$, then the image of eq 1 is not ideal, limited by the spatial resolution of $\delta \sim b/(-\ln|\epsilon + 1|) \geq b/\ln Q$, where $Q = -\mathrm{Re}\epsilon/\mathrm{Im}\epsilon$ is the quality factor of the plasmon resonance of the metal. The highest value of $Q \sim 100$ for any natural material from the near-infrared to ultraviolet region is for silver for light frequency $\hbar\omega \approx 1.2$ eV. The surface plasmon resonance would have shifted to this frequency if the values of host dielectric constant $\epsilon_h \sim 100$ were available. However, it is not the case, and the realistic values of $\epsilon_h \approx 12$ are typical for wide-band semiconductors (e.g., $Al_{0.2}Ga_{0.8}As$)[9] for $\hbar\omega$

10.1021/nl047957a CCC: $30.25
Published on Web 01/22/2005

= 2.2 eV. This choice provides the best possible suppression of the absorption adverse effects.

Now we consider a principally different source of the lens imperfection, namely *spatial dispersion*, or *nonlocality* of the dielectric response function $\epsilon(\omega,\mathbf{k})$ that depends not only on frequency ω but also on wave vector $\mathbf{k}$. In metals, the characteristic wave-vector scale of $\epsilon(\omega, k)$ is $k \sim w/v_F$, where v_F is the electron velocity at the Fermi surface. For $k \geq |\omega|/v_F$, there exists the Landau damping that additionally contributes to the optical losses described by $\mathrm{Im}\epsilon(\omega, k)$.[10]

For such a spatially dispersive dielectric function, we should carefully reformulate the boundary conditions for ballistic electrons at the surface of the metal. We will consider density of electrons in the metal as constant neglecting the narrow (width on order of the Debye screening radius $r_D \sim 0.1$ nm) Schottky layer in the metal at the interface. We assume that the semiconductor of the embedding medium is undoped and neglect Schottky-layer electric fields inside the semiconductor, because they are too weak to change its dielectric function. We also neglect the Friedel oscillations[10] because their period is too short, $\sim 1/k_F \sim 0.1$ nm, where k_F is the electron wave vector at the Fermi surface.

To take into account the effect of boundaries, we assume specular reflection of electrons from the surface. As was shown in ref 11, the ideal specular reflection implies that a nonlocal electrostatic problem for a half-infinite metal is equivalent to a problem in bulk metal

$$\nabla(\hat{\epsilon}\nabla\varphi_i) = 2E_\perp(x, y, 0)\,\delta(z) \tag{3}$$

where $E_\perp(x, y, 0)$ is the normal electric field at this surface, φ_i is the field potential in the metal, and $\hat{\epsilon}$ is the nonlocal dielectric response operator. The Dirac delta function emulates the boundary condition at the metal surface.

For the slab, an electron experiences multiple reflections from both its surfaces. To correspondingly generalize eq 3, we reflect each boundary periodically in each other. As a result, the potential φ_i satisfies an equation

$$\nabla(\hat{\epsilon}\nabla\varphi_i) = 2\sum_{n=-\infty}^{\infty}\left\{E_\perp^L(x, y, 0)\,\delta(z - 2bn) - E_\perp^R(x, y, b)\,\delta\left[z - 2b\left(n + \frac{1}{2}\right)\right]\right\} \tag{4}$$

where $E_\perp^L(x, y, 0)$ and $E_\perp^R(x, y, b)$ are the electric fields at the left and right faces of the slab.

The solution of eq 4 yields a periodic potential of period $2b$ in the z direction with discontinuities of the normal electric field $2E_\perp^L(x, y, 0)$ at $z = 2nb$ and $2E_\perp^R(x, y, b)$ at $z = (2n + 1)b$. In the $\mathbf{k}$ space

$$\varphi(\mathbf{k}) = \frac{2}{k^2\epsilon(\omega, k)}\sum_{n=-\infty}^{\infty}\{E^L(k_r)\exp(2ik_z nb) - E^R(k_r)\exp[i(2n + 1)k_z b]\} \tag{5}$$

where $E^L(k_r)$ and $E^R(k_r)$ are the 2D Fourier transforms of $E_\perp^L(x, y, 0)$ and $E_\perp^R(x, y, b)$. Deriving eq 4, we have taken into account the cylindrical symmetry of the problem. This potential should be found consistently with the potentials outside of the metal slab, where they obey the Laplace equation whose solutions to the left (L) and right (R) of the slab are

$$\varphi^L(k_r, z) = \alpha^L(k_r)\exp(k_r z) + \beta^L(k_r)\exp(-k_r z)$$
$$\varphi^R(k_r, z) = \alpha^R(k_r)\exp[k_r(z - b)] + \beta^L(k_r)\exp[-k_r(z - b)] \tag{6}$$

From eq 5, performing the inverse Fourier transform over k_z, we express the continuity equation for the left face of the metal slab as

$$\alpha^L(k_r) + \beta^L(k_r) = \frac{1}{k_r}[uE^L(k_r) - vE^R(k_r)] \tag{7}$$

where

$$u = \frac{k_r}{\pi}\sum_{n=-\infty}^{\infty}\int_{-\infty}^{\infty}\frac{\exp(2ik_z nb)}{k^2\epsilon(\omega, k)}\,\mathrm{d}k_z$$
$$v = \frac{k_r}{\pi}\sum_{n=-\infty}^{\infty}\int_{-\infty}^{\infty}\frac{\exp[ik_z(2n - 1)b]}{k^2\epsilon(\omega, k)}\,\mathrm{d}k_z \tag{8}$$

Similarly for $z = b$ (the right face of the slab), we get

$$\alpha^R(k_r) + \beta^R(k_r) = \frac{1}{k_r}[vE^L(k_r) - uE^R(k_r)] \tag{9}$$

The other two equations come from the displacement matching,

$$E^L(k_r) = \epsilon_L k_r[\alpha^L(k_r) - \beta^L(k_r)]$$
$$E^R(k_r) = \epsilon_R k_r[\alpha^R(k_r) - \beta^R(k_r)] \tag{10}$$

where ϵ_L and ϵ_R are the host dielectric permittivities to the left and right of the lens (metal slab).

Solving eqs 7, 9, and 10 for α_R and β_R, we get

$$\begin{pmatrix}\alpha^R\\ \beta^R\end{pmatrix} = \hat{T}\cdot\begin{pmatrix}\alpha^L\\ \beta^L\end{pmatrix} \tag{11}$$

where $\hat{T}$ is a 2×2 transfer matrix with matrix elements

$$T_{11} = [(v^2 - u^2)\epsilon_R\epsilon_L + u(\epsilon_R + \epsilon_L) - 1]/(2v\epsilon_R)$$
$$T_{12} = [(u^2 - v^2)\epsilon_R\epsilon_L + u(\epsilon_R - \epsilon_L) - 1]/(2v\epsilon_R)$$
$$T_{21} = [(v^2 - u^2)\epsilon_R\epsilon_L + u(\epsilon_R - \epsilon_L) + 1]/(2v\epsilon_R)$$
$$T_{22} = [(u^2 - v^2)\epsilon_R\epsilon_L + u(\epsilon_R + \epsilon_L) + 1]/(2v\epsilon_R) \tag{12}$$

This transfer matrix, $\hat{T}(\epsilon_L, \epsilon_R)$, has the following general properties:

$$\sigma_x \hat{T}(\epsilon_L, \epsilon_R)\sigma_x = [\hat{T}(\epsilon_R, \epsilon_L)]^{-1}$$
$$\det[\hat{T}(\epsilon_L, \epsilon_R)] = \epsilon_L/\epsilon_R \quad (13)$$

where σ_x is a Pauli matrix.

Consider a system of charges to the left of the lens as the source of the fields (no charges are to the right of it). Then the field to the right of the lens is given by eq 6 where $\alpha_R = 0$ and β_R is explicitly given by

$$\beta_R = [(\hat{T}^{-1})_{22}]^{-1}\beta_L \quad (14)$$

For a unit charge at the point (0, 0, $-a$), $\beta_L(k_r) = 8\pi \exp(-k_r a)/k_r$. Due to the linearity of the problem, this, along with eq 14, provides its general solution for any charge distributions to the left of the lens. Note that the problem solved is generally dynamic, i.e., time dependent, as described by the dependence on ω.

There is also interest in the problem of eigenmodes [surface plasmons (SPs)], see, e.g., ref 12, which is defined by eq 11 for $\alpha_R = \beta_L = 0$. From this, we obtain an equation for eigenfrequencies of surface plasmons

$$T_{22}[\epsilon(\omega, k); \epsilon_L, \epsilon_R] = 0 \quad (15)$$

where a functional dependence on $\epsilon(\omega, k)$ is indicated.

To simplify eq 8, we adopt conditions realistic for $b \gtrsim 5$ nm: $b \gg v_F/\omega$ and $k_r \ll \omega/v_F$; for instance, $v_F/\omega \approx 0.5$ nm for $\hbar\omega = 2.2$ eV. Then the integrands are rapidly oscillating functions for $n \neq 0$, and the integrals can be evaluated using a stationary phase method:

$$u = \frac{1}{\epsilon(\omega, 0)}\left[\frac{1}{\tanh(bk_r)} - k_r c(\omega, k_r)\right]$$
$$v = \frac{1}{\epsilon(\omega, 0)}\frac{1}{\sinh bk_r}$$
$$c(\omega, k_r) \equiv \frac{1}{\pi}\int_{-\infty}^{\infty}\left[\frac{\epsilon(\omega, 0)}{\epsilon(\omega, k)} - 1\right]\frac{dk_z}{k^2} \quad (16)$$

For the case of unit charge and $\epsilon_L = \epsilon_R \equiv \epsilon_h$, from eqs 6, 14, and 16, we obtain an explicit solution

$$\beta_R(k_r) = 8\pi k_r^{-1}\epsilon(\omega, 0)\exp[-k_r(a-b)] \times$$
$$\{[\epsilon_h + \epsilon(\omega, 0) - \epsilon_h k_r c(\omega, k_r)]^2 \exp(2k_r b) - [\epsilon_h - \epsilon(\omega, 0) + \epsilon_h k_r c(\omega, k_r)]^2\}^{-1} \quad (17)$$

Note that $\epsilon(\omega, 0)$ can be taken directly from experiment.[5] From this, we can obtain an estimate for spatial resolution δ of the lens with logarithmic precision

$$\delta \sim \frac{2b}{|\ln[Q^{-2} + |c(\omega, 0)/b|^2]|} \quad (18)$$

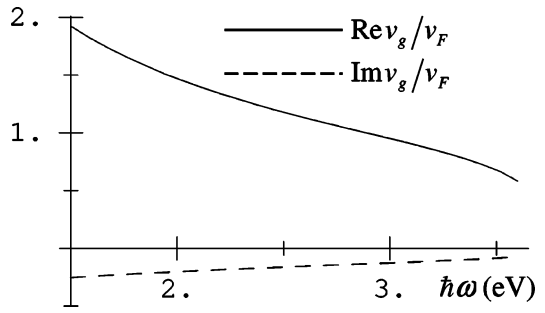

Figure 1. Group velocity of surface plasmons as a function of frequency in units of Fermi velocity. Solid and dashed curves correspond to the real and imaginary parts.

The function $c(\omega, 0) \sim v_F/\omega$ dominates δ for $b \lesssim 5$ nm, which is an effect of the SP dispersion and the related Landau damping. The same function, $c(\omega, 0)$, also determines dispersion relation (15) of SPs, which for $k_r b \gg 1$ is

$$\omega^2(k_r) \approx \omega_{sp}^2\left[1 + \frac{\epsilon_h k_r c(\omega, 0)}{1 + \epsilon_h}\right] \quad (19)$$

where ω_{sp} is the surface-plasmon frequency (for $k \to 0$). From this, it is clear that $c(\omega, 0)$ determines also group velocity of SPs $v_g = \omega c(\omega, 0)\epsilon_h/[2(1 + \epsilon_h)]$. From experimental data, which are available for SP frequency of $\hbar\omega = 3.67$ eV at metal/vacuum interface, we extract the values of v_g and find $c(\omega, 0)$: $c(\omega, 0) = 0.17 - i0.11$ nm.[13] Microscopic calculations[14] based on Kohn effective potential give negative value of the real part, $c(\omega, 0) = -0.11 - i0.24$ nm. A variational approach[15] yields $c(\omega, 0) = -0.07 - i0.08$ nm.

In light of inconsistency of these data and the fact that our frequencies are much lower, we invoke below the well-known Klimontovich−Silin−Lindhart formula[10,16]

$$\epsilon(\omega, k) = 1 + \frac{3\Omega_e^2}{k^2 v_F^2}\left[1 - \frac{\omega}{2kv_F}\ln\frac{\omega + kv_F}{\omega - kv_F}\right] \quad (20)$$

where electron plasma frequency $\Omega_e = \sqrt{4\pi N_e e^2/m}$, N_e is the electron density, e is the elementary charge, m is electron effective mass, and v_F is the Fermi velocity of electrons. Complex function $\ln(u)$ is defined as $\ln(u) = \ln|u| - i\pi$ for $u < 0$. Equation 19 is identical to the corresponding result of the random phase approximation (RPA), which is expected to work well in our case when $\omega \ll \Omega_e$ and $k \ll k_F$. This formula satisfies general properties of the spatial-dispersive dielectric response; in particular, it describes Landau damping for $k \geq \omega/v_F$.

From eq 19, we find and show in Figure 1 the real and imaginary parts of v_g. The imaginary part is small enough, which indicates that SPs are well-defined excitations. For $\omega = \omega_{sp}$, from these data we find $c(\omega, 0) = 0.44 - i0.053$, which has correct sign but overestimates $Rec(\omega, 0)$ with respect to the experiments discussed above. However, we expect that RPA works better for the computations presented below, which are done at a lower frequency of $\hbar\omega = 2.2$ eV for silver.

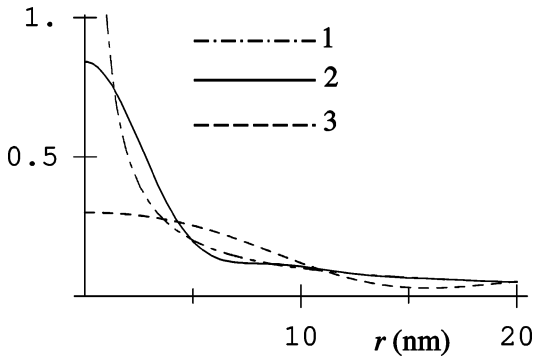

Figure 2. Electric potential of the image (in arbitrary units) in the focal plane $z = 2b - a$ of the metal slab lens for $\hbar\omega = 2.2$ eV as function of distance r from the image point of (0, 0, $2b - a$). The dash−dot curve (1): ideal image [the potential of a real charge at a point (0, 0, $2b - a$)]. The solid curve (2): image of a charge at a point (0, 0, $-a$) obtained without the spatial dispersion for the experimental value of $\epsilon(\omega, 0)$. The dashed curve (3): image of the same charge with the spatial dispersion taken into account, obtained from eqs 6, 16, 17, and 20. Thickness of the slab $b = 5$ nm.

To demonstrate the principal limitations imposed by the spatial dispersion of the dielectric response of metals on spatial resolution of a metal slab lens, we show in Figure 2 the images of a unit charge position to the left of the lens at a point (0, 0, $-a$) as distributions of the electric field potential in the image plane of $z = 2b - a$. We have chosen the lens slab thickness to be reasonably small, $b = 5$, nm to make manifest the effects of the spatial dispersion. Without a spatial dispersion taken into account, we show the image of a charge by a solid curve. This image practically coincides with the ideal image of a charge at the image point of (0, 0, $2b - a$) for distances from the image center $r \geq 2$ nm. In sharp contrast, if the spatial dispersion is taken into account using eqs 6, 16, 17, and 20, then the corresponding potential distribution shown by the dashed curve in Figure 2 deviates significantly from the ideal image (the dash−dot curve) at all distances in the graph. At distances $r < 5$ nm, this deviation becomes dramatic. We have checked that for $b =$ 10 nm such deviations become much smaller (data not shown), as expected from eq 17.

For nanolithography applications, it is important that the lens reproduces images of more complex objects. One of such objects often used for testing is a thin light-emitting washer that we model as an annulus of uniform optical polarization (oscillating dipoles). The image on the other side from the silver slab lens for the case of no spatial dispersion is shown in Figure 3a. The washer is nearly perfectly reproduced in the image plane, the contrast is high, and the edges are weakly smeared out ($\lesssim 2$ nm). In contrast, the image for the case of spatial dispersion taken into account (Figure 3b) shows low contrast and very significant smearing out. In particular, the intensity in the center of the washer is $\approx 60\%$ of the maximum intensity; the smearing of the edges is $\gtrsim 5$ nm. Thus, the spatial dispersion of the interacting electron liquid in the metal has a pronounced deteriorating effect on the nanoimage quality on the scale of 5 nm or less.

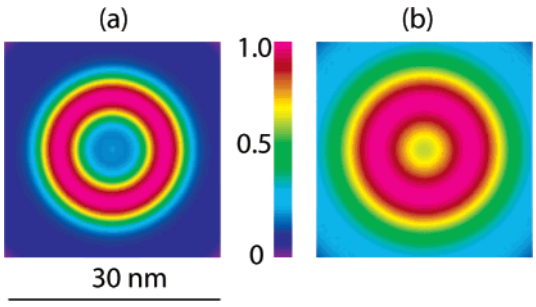

Figure 3. Images of washer (annulus) with the external radius 10 nm and internal radius 5 nm for the case of no spatial dispersion (a) and spatial dispersion taken into account (b). This washer carries a uniform distribution of dipole emitters at $\hbar\omega = 2.2$ eV polarized in the z direction. The light intensity of the images is shown in the focal plane by color coding (arbitrary units).

To briefly discuss the results obtained, using a semiconductor environment to shift the surface plasmon frequency toward the red spectral region, we suggest to dramatically reduce losses and increase the resolution of the lens to the order of nanometers. We have shown that at such distances the main mechanism limiting the resolution of the metal slab lens is the spatial dispersion of the dielectric response of the Fermi liquid of interacting electrons in the metal. For a thin silver slab, this effect limits resolution to ~5 nm. One of the goals of this letter is to stimulate measurements of the metal lens' nanoimaging and surface plasmons' spatial dispersion that limits the nanoimage resolution.

The possible applications of our theory include the nanoimaging and nanolithography in the extreme nanolimit, where the size of objects and images is ~5 nm. Such resolutions are predicted for "solid-state immersion" where the metal slab is surrounded by a semiconductor of high enough dielectric permittivity. In such applications, the metal slab protects the modified surface from the direct contact with the light aperture. Another similar application is the protection of a nanolithographic mask. In the problems of nanospectroscopy and ultramicroscopy, the slab lens spatially separates the probe and object, which, in particular, prevents their chemical interaction, e.g., damage by the oxygen in a biological object. Imaging of semiconductor nanostructures is another application that may allow for the direct imaging of their electron wave functions.

Acknowledgment. This work was supported by the Chemical Sciences, Biosciences and Geosciences Division of the Office of Basic Energy Sciences, Office of Science, U.S. Department of Energy. Partial support came from the U.S.−Israel Binational Science Foundation.

References

(1) Veselago, V. G. *Sov. Phys. Uspekhi* **1968**, *10*, 509−514.
(2) Smith, D. R.; Padilla, W. J.; Vier, D. C.; Nemat-Nasser, S. C.; Schultz, S. *Phys. Rev. Lett.* **2000**, *84*, 4184−4187.
(3) Pendry, J. B. *Phys. Rev. Lett.* **2000**, *85*, 3966−3969.
(4) Lagarkov, A. N.; Kissel, V. N. *Phys. Rev. Lett.* **2004**, *92*, 077401-1−4.
(5) Johnson, P. B.; Christy, R. W. *Phys. Rev. B* **1972**, *6*, 4370−4379.
(6) Ramakrishna, S. A.; Pendry, J. B. *Phys. Rev. B* **2003**, *67*, 201101-(R).

(7) Haldane, F. D. M. Electromagnetic Surface Modes at Interfaces with Negative Refractive Index Make a "Not-Quite-Perfect" Lens. In *arXiv: cond-mat/0206420*; 2002.
(8) Batygin, V. V.; Toptygin, I. N. *Problems in Electrodynamics*; Academic Press: London, 1964.
(9) Aspnes, D. E.; Kelso, S. M.; Logan, R. A.; Bhat, R. *J. Appl. Phys.* **1986**, *60*, 754−767.
(10) Mahan, G. D. *Many-Particle Physics*; Kluwer Academic: New York, 2000.
(11) Wilkinson, M.; Mehlig, B. *J. Phys.: Condens. Matter* **2000**, *12*, 10481−10498.
(12) Stockman, M. I.; Faleev, S. V.; Bergman, D. J. *Phys. Rev. Lett.* **2001**, *87*, 167401-1−4.
(13) Rocca, M.; Biggio, F.; Valbusa, U. *Phys. Rev. B* **1990**, *42*, 2835−2841.
(14) Feibelman, P. J. *Phys. Rev. B* **1974**, *9*, 5077−5098.
(15) Beck, D. E.; Celli, V. *Phys. Rev. Lett.* **1972**, *28*, 1124−1126.
(16) Lifshitz, E. M.; Pitaevskii, L. P. *Physical Kinetics*; Pergamon Press: New York, 1981.

NL047957A